A New Concept of Energy Absorbing System for the Double Hull Tanker

J. W. Lee[1], H. Petershagen[2], J. Rörup[2], J. Y. Kim[1], J. H. Yoon[3]

[1] Inha University, 402-751 Inchon, Korea
[2] Univ. Hamburg-Harburg, Lämmersieth 90, 22305 Hamburg, Germany
[3] Samsung Heavy Industries, 656-800, Koje, Kyungnam, Korea

Abstract

A new concept of collision energy absorbing system for the New Oil-tankers with Advanced Double Hull Structure(NOAHS and NOAHS II) are presented through the joint-research program between Inha and Hamburg-Harburg University. A comparative study on collision resistance of these proposed side structures with standard double hull structure of 310K DWT class VLCC, is carried out. The fatigue investigation of structural detail parts is also included. It contains a comparative fatigue study based on pertinent regulations of Classification Societies.

Keywords : VLCC, double hull structure, energy absorption, flexible structure, fatigue strength

1 Introduction

Recently, the structural design of oil tankers has drawn a keen interests and several proposals are presented, based on the collision resistance of the structures. Collision resistance of oil-tanker involves basically two major areas; the structural behavior of the double side hull structure with its components and the rigidity of colliding bow structure. As the installation of soft bow structure is far from the practical application, it seems more attractive to improve the energy absorption capacity of double hull structure. Based on the joint research program on the development of double hull structure of oil-tanker between Inha and Hamburg-Harburg university, two types of new oil-tankers with advanced double hull structure(NOAHS and NOAHS II) are presented to demonstrate the crashworthiness and a comparative study of these types of new oiltankers is carried out with a standard double hull structure of 310K DWT VLCC. Finally, according to the pertinent regulation of two Classification Society, GL and DNV, the fatigue strength of structural detail parts is also investigated.

2 New Oil Tanker with Advanced Double Hull Structure (NOAHS & NOAHS II)

The midship tank structure of standard 310K DWT VLCC is shown in Figure 1, which gives the reference collision resistance against side collision. The main characteristics of standard VLCC
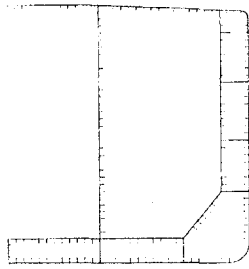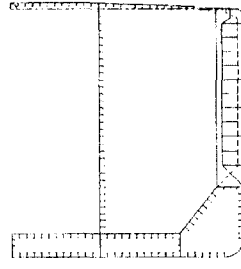
Figure 1. Midship section of standard VLCC.

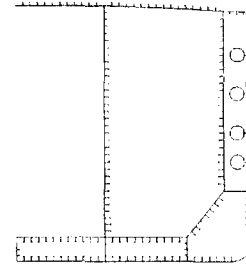**Figure 2.** Midship section of NOAHS.

Figure 3. Midship section of NOAHS II.

and new proposed VLCC are listed in Table 1.

One type of advanced double hull structure(NOAHS) is composed of crushing and tension plate strips of $11.5mm$ thickness, which are arranged alternatively in vertical direction as shown in Figure 2. The transverse structure of the double side hull consists of an alternate arrangement of frames on the side shell "side frames" and on the side longitudinal bulkhead "inner frames". A side frame is part of a transverse ring "trans ring", which extends over the whole ship breadth, except the side longitudinal bulkhead. The additional inner frames, which exist only in the double side hull, stiffen the side longitudinal bulkhead. The inner frames are located at a distance of half a frame spacing from the trans rings. The inner frames and the shell frames have a floating small web depth and large flange width. Five tween-decks in the double side hull act as "collision crushing members" and between the shell frames and the inner frames extend four stringers acting as "collision tension spring members", which should act collision energy absorbing system of "NOAHS". The another type of proposed double hull structure is "NOAHS II", which is composed of four large tubes in vertical direction with $1800mm$ diameters and $40mm$ thickness, as shown in Figure 3. The numerical simulation for ship collision and crushing damage of the hull structures are carried out, where the crushing behavior of the plate and tube members in energy absorbing process are analyzed and tested[Lee et al., 1996, Kim et al., 1998, & Lee, Petershagen et al., 1998 & Lee, Shim, 1998].

Table 1. Characteristics of standard and new VLCC.

Width of Double Side	$3380mm$
depth of Double Bottom	$3000mm$
Transverse Spacing	$5080mm$
Floor Spacing	$5080mm$
Typical Longi. Stiff. Spacing	$900mm$
Material of Deck Structure	YP320 HT Steel
Material of Double Side Structure	Mild Steel
Material of Inner Bottom Structure	Mild Steel
Material of Bottom Structure	YP320 HT Steel

3 Collision Energy of Structural Members

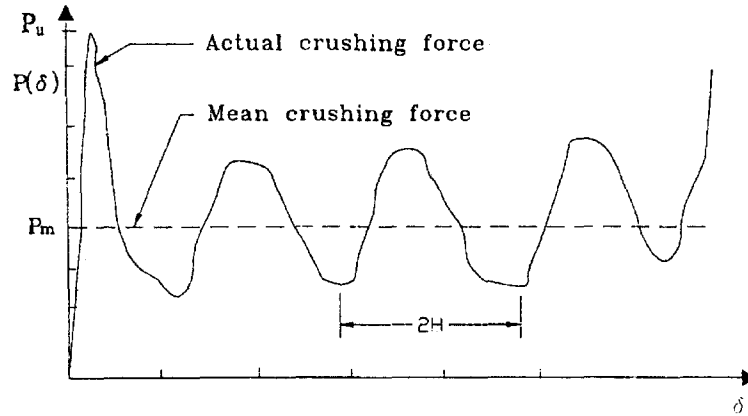## 3.1 Crushing Energy of Plates

Figure 4. Force-shortening characteristic of an axially compressed box column.

The absorbed energy of thin-walled structure under axial load $P(\delta)$ can be expressed by integration of $P(\delta)$ over the crushing distance δ.

$$E = \int_0^\delta P(\delta)d\delta \tag{1}$$

When the mean crushing strength is introduced, equation(1) can be presented as

$$E = P_m\delta \tag{2}$$

The mean crushing load P_m is generally dependent on the ultimate buckling strength of the plate, which is characterized by the geometry and material properties of the plates, i.e., thickness t, width b, length l, yield stress σ_y, elastic modulus E and boundary conditions α_i, which is denoted by the vertical deflection and rotation angle of edges in radian. Then, the mean crushing load P_m can be expressed as follows.

$$P_m \propto f(t, b, l, \sigma_y, E, \alpha_i) \tag{3}$$

where, the function f is understood as the ultimate buckling strength, P_u of the plate. By applying the Π- theorem for dimensional analysis, energy dissipation equation for whole crushing length of plates can be formulated by

$$E = C \cdot \sigma_y \cdot t^2 \cdot \delta \tag{4}$$
$$= C \cdot \sigma_y \cdot t^2 \cdot b \cdot m$$

where,

$$C = \phi\{\tfrac{b}{t}\sqrt{\tfrac{\sigma_y}{E}} \ , \ \tfrac{\alpha_i}{l}\} = \phi\{\tfrac{b}{t} \ , \ \tfrac{\alpha_i}{l}\} \qquad \text{for unit strain}$$

$$\delta = b \cdot m = \delta_u \cdot m \qquad \text{for whole crushing length } l = \delta$$

When we introduce a unit crushing length $\delta_u = 2H$ as shown in Figure 4, C can be understood as a variable coefficient which is dependent on plate slenderness b/t and m is the number of lobes with unit length δ_u.

$$m = \frac{l}{\delta_u} \tag{5}$$

where, l is the initial height of the plate.

Under the assumption of symmetric collapse mode, which is verified experimentally and theoretically, unit length is given by

$$\delta_u = 2\sqrt[3]{b^2 \cdot t} \tag{6}$$

The effective unit length δ_{eff} will be adopted as 70% of initial unit length for unstiffened plate from experimental results.

$$\delta_{eff} = 1.4\sqrt[3]{b^2 \cdot t} \tag{7}$$

$$m_{eff} = \frac{l_{eff}}{\delta_{eff}} \tag{8}$$

Let slenderness ratio $\frac{b}{t}$ be denoted by β, then C is function of β; $C = f(\beta)$. By using the experimental data of unstiffened box column[Lee, 1981], a proper relationship between C and β is obtained as follows

$$C = 0.7622\sqrt{\beta} + 14.911 \tag{9}$$

Therefore the dissipation energy of the unstiffened plate is expressed by

$$E = (0.7622\sqrt{\beta} + 14.911) \cdot \sigma_y \cdot t^2 \cdot b \cdot m_{eff} \tag{10}$$

And the similar expressions for the stiffened plates are obtained[Lee, 1996].

3.2 Crushing Energy of Tubes

The crushing energy of a tube due to compression can be evaluated with the following formula[Tore, 1981].

if $\quad w \le d$

$$\frac{P}{P_o} = \sqrt{1 - \frac{w^2}{d^2}} + \frac{w}{d}\sin^{-1}\left(\frac{w}{d}\right) \tag{11}$$

$$U = P_o d\left(\frac{3}{4}\frac{w}{d}\sqrt{1 - \frac{w^2}{d^2}} + \frac{1 + 2\frac{w^2}{d^2}}{4}\sin^{-1}\left(\frac{w}{d}\right)\right) \tag{12}$$

Table 2. The six different type of tubes with a constant weight.

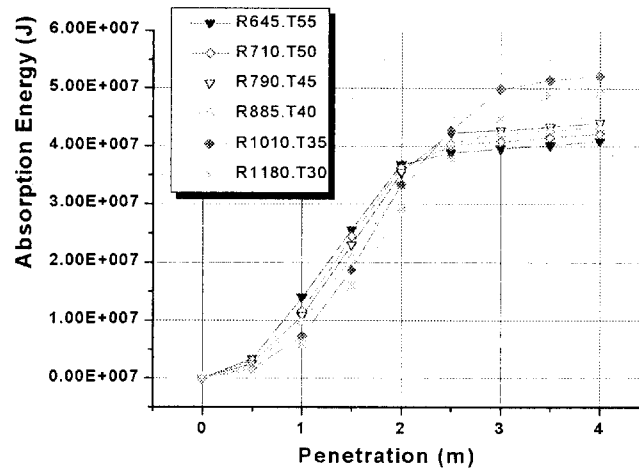| Thickness (mm)	30	35	40	45	50	55
Radius (mm)	1080	1010	885	790	710	645

Figure 5. Energy absorption according to the variation of Radius(R) and Thickness(T) of tubes of constant weight.

if $w > d$

$$\frac{P}{P_o} = \frac{\pi}{2}\frac{w}{d} \tag{13}$$

$$U = \frac{\pi}{8}P_o d\left(1 + 2\frac{w^2}{d^2}\right) \tag{14}$$

In order to find out the optimal dimension of the tube, the simulation of only the tube as collision resistance member is carried out. The six different type of tubes in thickness and diameters with a constant weight as shown in Table 2 are analyzed to get the maximum collision energy.

From the Figure 5, the tube with a diameter $1010mm$ and thickness $35mm$ shows the efficient behaviour in energy absorption. And to find out the optimal arrangement of tube in the double hull space of a tanker, three different positions are adopted, namely

· Position I : The outer position in the side frames
· Position II : The middle position between the side frames and the inner frames
· Position III : The inner position in the inner frames

As shown in Figure 6, the position I of the tube arrangement gives the maximum energy absorption due to collision until the rupture of inner bulkhead[Kim et al., 1988].
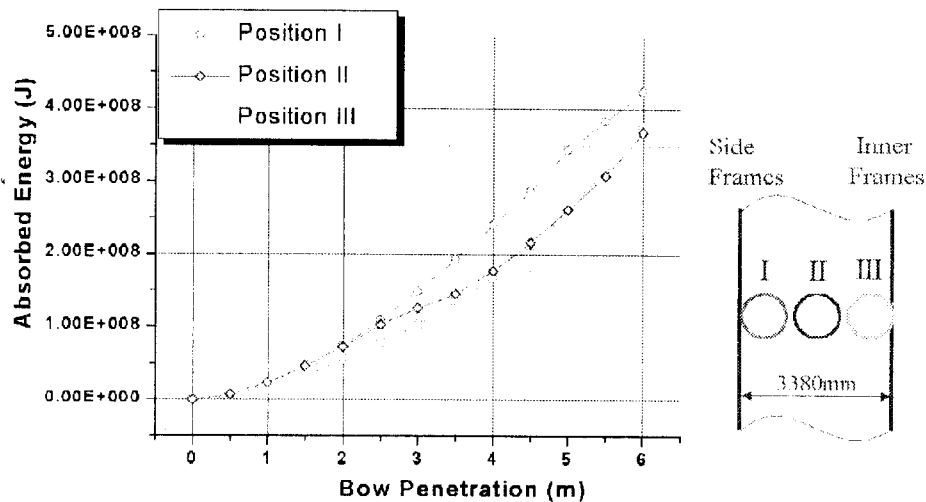
Figure 6. Energy absorption according to the position of tube arrangement.

Table 3. Principal dimensions of two ships in collision scenario.

Principal dimensions		Struck ship	Striking ship
Length	$[m]$	318	264
Breadth	$[m]$	58	47.8
Depth	$[m]$	31.25	22.8
Draft	$[m]$	21.4	14.6
Displacement	$[ton]$	310,000	150,000

4 Evaluation of Collision Resistance

4.1 Collision Scenario

Striking ship collides the center of struck ship's normally. The principal dimensions of two ships which are participated in collision scenario, are listed in Table 3. Struck ship's displacement is 310K DWT and striking ship's one is 150K DWT Tanker in ballast condition. Observing the object of this study; the development of efficient hull structure in energy absorption, we adopt the orthogonal collision case, as collision scenario. We select two different cases in collision point of the struck ship, NOAHS, as follows.

- Case 1: Striking ship collides directly against center of side frame of NOAHS
- Case 2: Striking ship collides directly against the midpoint of two side frames of NOAHS

In this case hydrodynamic force is neglected, due to the simplification of structural analysis of developed struck oil-tanker. In the analysis, struck ship is modeled by one tank length, and total number of the elements are approx. 16,000. In the striking ship, bulbous bow assumes rigid, rid of all inner elements. Struck ship is assumed in fully loaded condition, move straight to the y-coordinate. Collision speed is set constant value of $10m/s$ for comparison with Kitamura's

result[Kitamura, 1996]. The orthogonal collision scenario of NOAHS II as a struck ship with 150K DWT is the similar case as NOAHS's one.
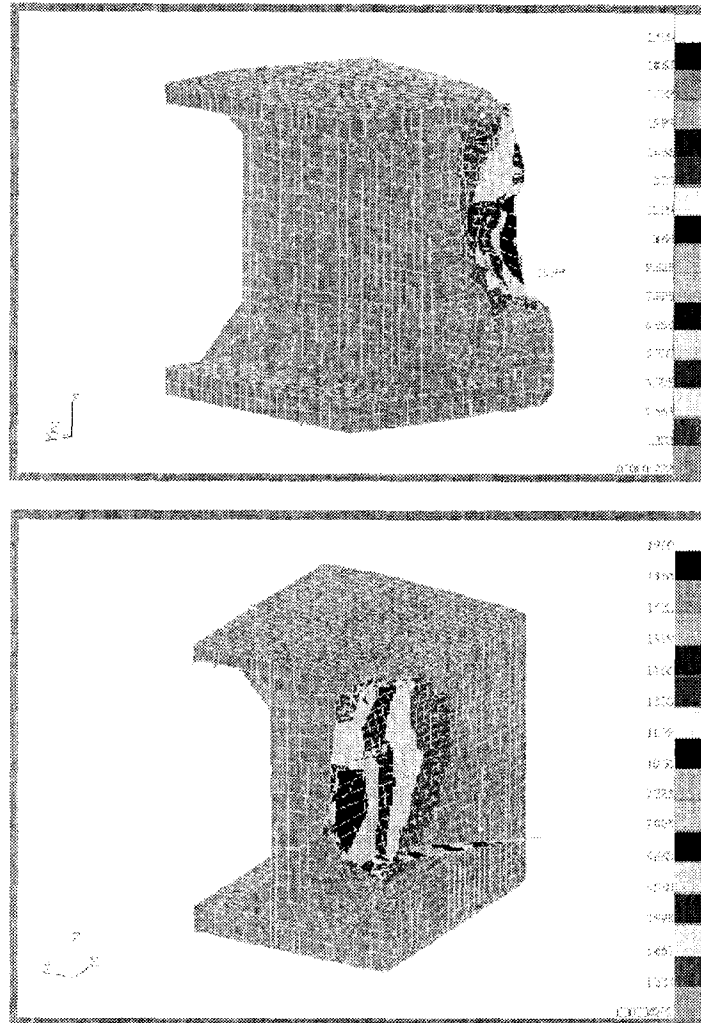

Figure 7. Side view of collision model.

4.2 Contact Force

We perform the numerical analysis of the proposed side structure models by using the software MSC/DYTRAN, as a explicit solution method. Side collision damages of NOAHS II at bow penetration of 6m are shown in Figure 7. The contact forces of new proposed oil-tanker, NOAHS and NOAHS II in Figure 8 and 9 show, at the initial stage, reltively lower magnitude than the contact forces of standard VLCC and Kitamura's proposed VLCC shown in Figure 10 and 11.

This phenomenon can be understood due to the flexible stiffness of side shell structure of NOAHS and NOAHS II oil-tanker. However, when the bow penetration approaches to 2m depth, the contact force of standard VLCC and Kitamura VLCC drops dramatically. In contrast to this
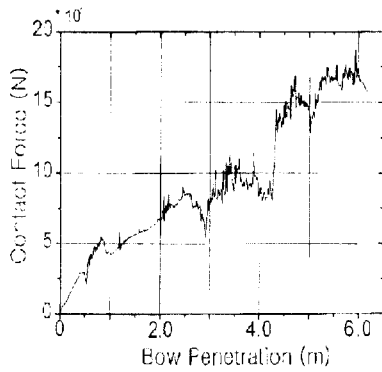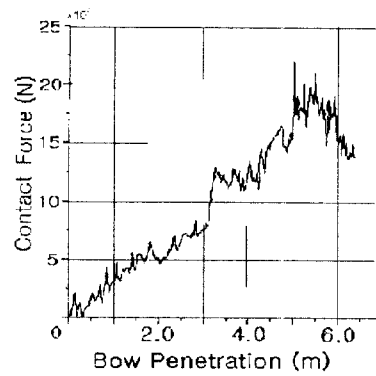
18

Figure 8. Contact forces of the struck ships(NOAHS).

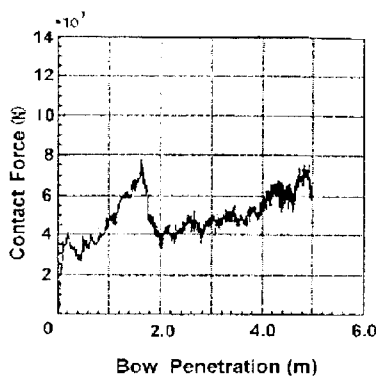**Figure 9.** Contact forces of the struck ships(NOAHS II).

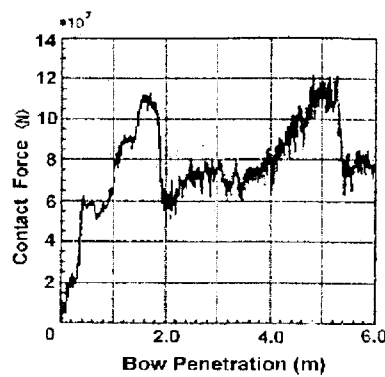**Figure 10.** Contact forces of the struck ships(Standard VLCC).

Figure 11. Contact forces of the struck ships(Kitamura VLCC).

behavior, the contact forces of NOAHS and NOAHS II increase steady until the rupture initiation of side shell begins at $2.5m$ for NOAHS and $2m$ for NOAHS II. Furthermore, in case of NOAHS II, the contact force increase quite a lot in magnitude over the bow penetration depth $3m$. This behavior is resulted from the effective performances of crushing tubes. At the bow penetration depth about $5m$, the contact forces of NOAHS and NOAHS II are still increasing due to the maintaining of rigidity of side structure, while the contact forces in the cases of standard and Kitamura VLCC drop rapidly due to the loss of side structure's rigidity. The maximum value of contact force of NOAHS is greater than that of standard VLCC by approx. 120% and that of Kitamura proposed VLCC by approx. 60%. The maximum penetration depth of approx. $6m$ for NOAHS and NOAHS II shows the rupture initiation of side longitudinal BHD, which gives much larger value that of other two cases. This phenomena is understood due to the global flexible effects of the proposed double hull structures. The initial rupture of side longitudinal BHD begins to lose capability of double hull structure for the prevention of oil spillage. Therefore, the collision analysis after the penetration depth of $6m$ needs not considered.
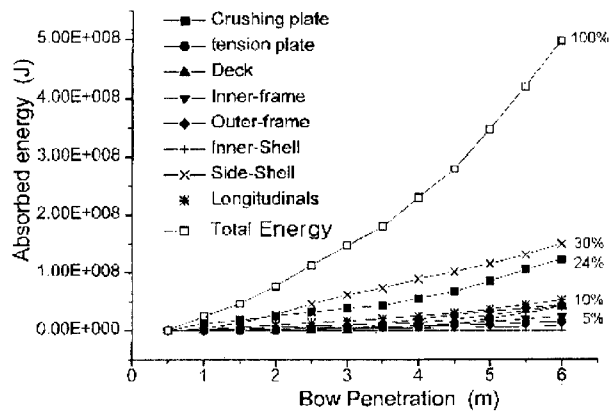
Figure 12. Energy absorption of structural members of proposed oil tankers(NOAHS).
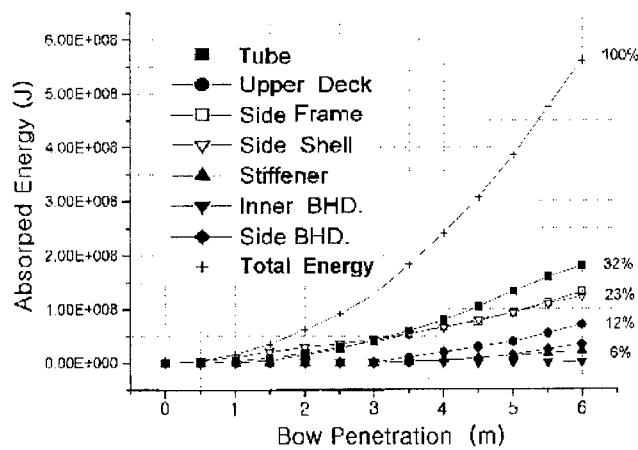

Figure 13. Energy absorption of structural members of proposed oil tankers(NOAHS II).

4.3   The structural absorbing energy

The collision energy for NOAHS II is absorbed in large quantity by side shell until the initial stage of penetration depth, $3m$. From this depth, the energy absorption of tube member is dominant as shown in Figure 12. And the structural members of side shell and crushing plate for NOAHS absorb the major parts of collision energy shown in Figure 13. For the comparison, we show the relationship between the total absorbed energy and bow penetration of four VLCC oil-tankers in Figure 14, where the total absorbed energy via. bow penetration depth of three cases is shown. NOAHS and NOAHS II have the larger collision absorption energy than the other VLCC after the penetration depth of approx. $5m$. Therefore it is understood that the proposed double hull tanker NOAHS II is more effective in the severe collisions.
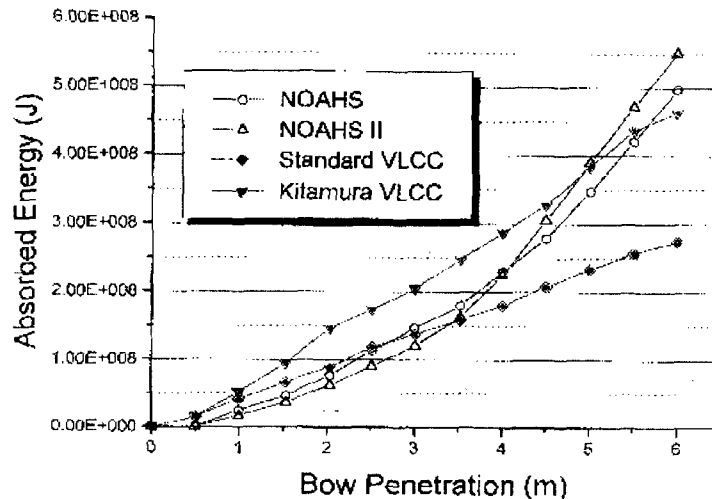
Figure 14. Comparison of absorbed energy.

5 Fatigue Strength

Fatigue details of the NOAHS-tanker were selected according to the consideration that the new design utilizes unconventional elements, amongst which the corrugated members play an important role. The transverse bulkheads have one corrugation close to the side longitudinal bulkhead(inner skin). This vertical extending corrugation is stiffened. The dominantly normal stress extends perpendicular to the corrugation and a bending moment is induced. This effect leads to stress concentration effects. Furthermore a fatigue assessment of the longitudinal end connections has been implemented. For VLCC's the longitudinal end connections are generally considered as a critical fatigue detail. Especially the side shell longitudinals in the region of the load water line are of interest.

The inner skin longitudinals have at the intersections with the transverse bulkheads only the half stiffener length. The local bending of this stiffener can induce only low stresses, but the stresses due to the relative deflection between bulkhead and adjacent transverse frame will be increased in case of a short stiffener length and a soft structure of the girder system without a strut in the wing tank.

The fatigue damage will be estimated for the first asymmetrical side shell stiffener (Z = 24.05m above Basis) and for the inner skin stiffener with the greatest relative deflection(Z = 19.55m above Basis).

The fatigue damage studies of these details have been carried out to the rules of Germanischer Lloyd[GL, 1997] and Det Norske Veritas [DNV, 1995 & DNV, 1993].

The concepts of the different classes differ in the methods of fatigue life assessment for structural details. The guidelines of the Classification Societies Det Norske Veritas(DNV) and Germanischer Lloyd(GL) are summarized here, partly by quotation of the corresponding rules.

5.1   The Rules of Det Norske Veritas(DNV)

The fatigue design is based on S-N curves corresponding to test results from smooth specimens without stress concentration and the notch stress range at the structural detail considered. The notch stress range is obtained by multiplication of the nominal stress by K-factors, which are given in [DNV, 1995]. The fatigue life may be calculated based on the S-N fatigue approach under the assumption of linear cumulative damage. Depending on the required accuracy of the fatigue evaluation it may be advisable to divide the design life into a number of time intervals due to different loading conditions and limitations of durability of the corrosion protection. S-N curves in air are often presented as bi-linear with a change in slope beyond 10^7 cycles. The use of bi-linear S-N curves complicates the expression for fatigue damage. In order to reduce the computational effort, simplified one-slope S-N curves have been derived for typical long-term stress range distributions. Use of the one-slope S-N curves leads to results on the safe side for calculated fatigue lives exceeding 20 years.

5.2   The Rules of Germanischer Lloyd(GL)

Corresponding to their notch effect, welded joints are classified into detail categories considering particulars in geometry and fabrication, including subsequent quality control, and definition of nominal stress. The S-N curves represent sectionwise linear relationships between $\log(\Delta\sigma)$ and $\log(N)$ with a change in slope beyond 5×10^6 cycles. To account for different influence factors, the design S-N curves have to be corrected for material effect, effect of mean stress, effect of weld shape and influence of importance of the structural element. The stress ranges $\Delta\sigma$ to be expected during the service life of the ship or structural component, respectively, are described by a stress range spectrum. Based on this spectrum and the S-N curve of the detail the fatigue life is calculated under the assumption of linear cumulative damage(Palmgren-Miner rule).
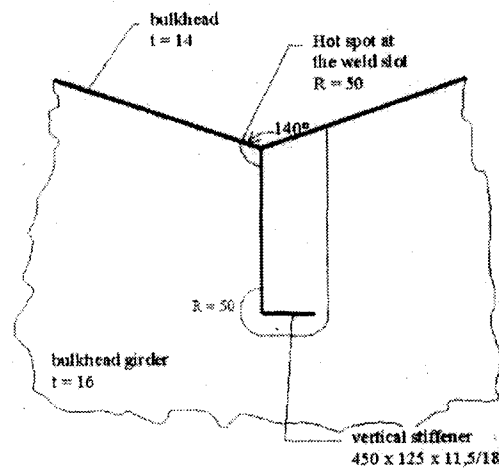

Figure 15. Top view of the bulkhead detail.

Table 4. Fatigue results at the bulkhead detail.

Classfication Society		GL	DNV	
Sailing route		North Atlantic	World wide	
Loading condition		Full	Full	Ballast
Fatigue stress range $[N/mm^2]$		**1256.6**	**1600**	**389**
Long term stress Distribution		$n = 5 \times 10^7$	$n = 5 \times 10^7$	
Weibull shape parameter		1.0	0.9144	
S-N curve Inverse Slope: m	for $n < 5 \times 10^6$	3	3	
	for $n > 5 \times 10^6$	5	3	
Reference stress rage for $n = 2 \times 10^6$		115.0	142.2	
Fatigue damage, D		**24.1**	**20.8**	

5.3 Fatigue of the Corrugation in the Transverse Bulkhead

The detail considered, see Figure 15, is a cut out in the bulkhead girder(Z = 22.25m above basis) for a vertical stiffener with a single-sided support(lug). The stiffener (450 $\times$ 125 $\times$ 11.5/18) is positioned on the corrugation of the bulkhead. The assessment is based on the structural stress at the detail considered. The structural stress is estimated by means of a local FE-model. The local model is loaded at its boundaries with displacements, computed with a global FE-model of the tank hold area. A detail description of this hot spot fatigue assessment is given in [Rörup, 1998].

The highest stresses are concentrated at the weld slot(R = 50mm) of the lug. The results of the fatigue assessment are listed in Table 4. With a fatigue damage of D = 20 and more the corrugation in the bulkhead is a very critical detail that has no safety against fatigue cracking in the considered condition.

The high stress range may be explained partly by the reduced size of the finite elements at the hot spot. But definitely the considered detail is very critical and it seems that improvements as a double-sided support for the vertical stiffener can not decrease the fatigue damage below one.

5.4 Fatigue of the Longitudinal End Connections

Figure 16 describes the design of the considered longitudinal end connections. The nominal stress, determined by simple engineering formulae, is the basis of this fatigue assessment. The total stress range is the composition of global stress induced to hull girder bending and the local stress.

The local stress is the sign right sum of the stress due to local bending of the longitudinal stiffener between supporting structures and the stress due to relative deflection of the nearest frame to a transverse bulkhead.

The relative deflection of the double hull is determined by a FE-model covering the midship tank and one half tank outside each end of the midship tank. The implemented calculations are taken from the report [GL, 1997].

This report describes the calculations in detail. The Rules of DNV consider that the sailing routes of oil-tankers correspond to a world wide operation. To compare the results with the GL-classification, which uses only the North Atlantic environment, the fatigue damage is calculated for operation in the North Atlantic. The fatigue damage increase of nearly factor 2 by changing the sailing route. Also in adjustment to the GL-classification the loads at 10^{-8} probability level of
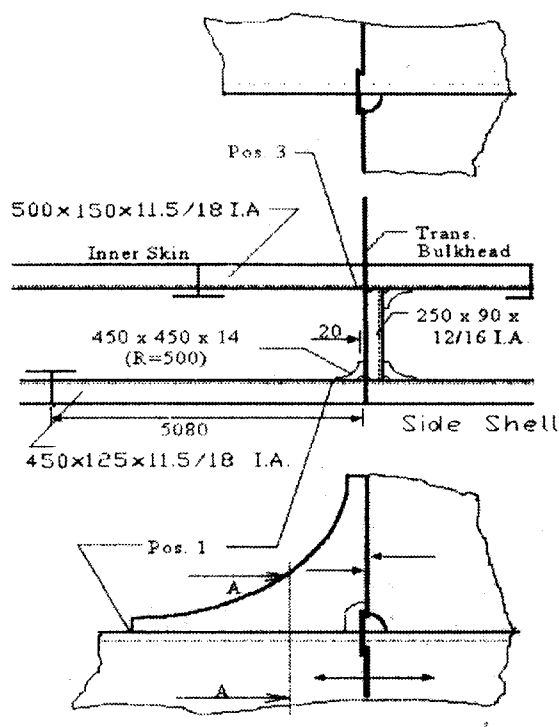
Figure 16. Top view of the stiffener details.

excess are used.

Generally DNV prefers the use of loads at 10^{-4} probability level of excess and above, because the fatigue damage is in this case not so sensitive to the estimated Weibull shape parameter.

Table 5 compares the details of the fatigue assessment. In the assessment to the rules of GL the relative deflection has a greater effect on the local stress range than to the rules of DNV. For both details this effect leads to a higher total stress range by an assessment to the GL-Rules. Especially at the inner skin stiffener(Position 3) the local stress range is mostly induced by the relative deflection. At Position 1 a higher fatigue damage results from the DNV-Rules and at Position 3 from the GL-Rules. Generally, for identical stress ranges, an assessment to the DNV-Rules results in a slightly higher fatigue damage than to the GL-Rules. But at Position 3 the very small stress range in the ballast condition decreases the total fatigue damage to the rules of DNV, while in the simplified assessment to the GL-Rules only the full loaded condition is considered. In respect of the fatigue damage at the considered longitudinal end connections the new tanker design is practicable. The fatigue damage at both details is clearly below one.

6 Conclusions

A comparative study of a new oil-tanker of crushing and tension plates (NOAHS) and tubes (NOAHS II) has been carried out with the conventional oil-tanker 310K and the other proposal. It has been shown that NOAHS II gives the largest value of the collision absorption energy, which

Table 5. Fatigue results at the longitudinal end connections.

	Position 1			Position 3		
Classification Society	GL	DNV		GL	DNV	
Loading condition	full	full	ballast	full	full	ballast
Pressure range $[kN/m^2]$	63.8	49.4	29.6	37.4	32.2	29.6
Stress range due to local bending	52.0	58.0	34.8	10.3	22.9	12.6
Stress range due to rel. deflection	86.8	26.8	-0.3	183.6	122.8	3.5
local stress range $[N/mm^2]$	**138.8**	**84.8**	**34.5**	**193.9**	**145.7**	**16.1**
Global stress range due to:						
- vertical hull girder bending	72.5	84.6	96.0	41.1	23.3	46.6
- horizontal hull girder bending	66.8	69.2	47.1	61.0	38.0	43.0
Global stress range $[N/mm^2]$	**139.3**	**153.8**	**143.1**	**102.1**	**61.3**	**89.6**
Total stress range(nominal)	**278.1**	**238.6**	**177.6**	**296.0**	**207.0**	**105.7**
Stress concentration	1.0	2.0	2.0	1.0	1.8	1.8
Fatigue stress range $[N/mm^2]$	**278.1**	**477.2**	**355.2**	**296.0**	**372.6**	**190.3**
Long term stress distibution, n	5×10^7	5×10^7		5×10^7	5×10^7	
Weibull shape parameter	1.0	0.904	0.878	1.0	0.9144	0.9144
S-N curve						
inverse slope, m — for $n < 5 \times 10^6$	3	3	3	3	3	3
inverse slope, m — for $n > 5 \times 10^6$	5	(one slope curve)		5	(one slope curve)	
reference stress range for $n = 2 \times 10^6$	88.0	142.2		104.0	142.2	
Fatigue damage, D	**0.60**	**0.69**		**0.40**	**0.29**	
Permissible stress range	322.0	474.0	497.7	380.6	467.6	467.6
Stress usage factor	**0.86**	**1.01**	**0.71**	**0.78**	**0.80**	**0.41**

is understood due to flexible effects of the global double hull structure systems. In respect of the fatigue damage at the corrugation in the bulkhead, the design of the NOAHS tanker should be reconsidered. However the double hull longitudinal end connection show quite practicable.

For the practical application, the detail design of NOAHS II should be investigated for further fatigue assessment.

Based on the numerical simulation system and experimental analysis for ship collision and crushing damage of the double hull structure, the optimum structure of double hull tanker will be presented.

Acknowledgments

References

1. Lee, J. W., Choung, J. M., 1996, Energy Dissipation and Mean Crushing Strength of Stiffened Plate in crushing, Journal of Hydro-space Technology, SNAK.
2. Kim, J. Y., Paik, H. Y., Lee, J. W., 1998, Collision Energy Absorption of Tube Members for Double Hull Structure, Proceedings of The 1998 KSSC Annual Summer Meeting, SNAK.
3. Lee, J. W., Petershagen, H. et al., 1998, Collision resistance and fatigue strength of New Oil-tanker with Advanced Double Hull Structure, The 7th PRADS, The Netherlands
4. Lee, J.W., Shim, C. S., 1998, Structural Arrangement of a Double Hull Tanker against Collision, R.I.S.T. Inha University
5. Paik, H. Y., Lee, J. W., 1997, Collision Energy Absorption of Side Hull Construction, Proceedings of The Annual Autumn Conference, SNAK.
6. Lee, J. W., Zur dissipationsenergie der isotropen platte, Dissertation, RWTH Aachen.
7. Tore, H. Söreide, 1981, Ultimate Load Analysis of Marine Structures, Tapir.
8. Kitamura, O., 1996, Comparative Study on Collision Resistance of Side Structure, International Conference on Designs and Methodologies for Collision and Grounding Protection of Ships, SNAME & SNAJ.
9. GL, 1997, Rules and Regulations, I - Ship Technology, Part 1: Seagoing Ships, Chapter 1 - Hull Structures, Germanischer Lloyd, Hamburg.
10. DNV, 1995, Fatigue Assessment of Ship Structures, Technical Report No.93-0432, Det Norske Veritas Classifications.
11. DNV, 1993, Rules for Classification of Ships, Part 3, Chapter 1, Hull Structure Design, Ships with Length 100 Meters and above, Det Norske Veritas, Hovik.
12. Rörup, J., 1998, Fatigue Strength of Oiltankers with Alternative and Conventional Double Hull Structure, Technische Universität Hamburg-Harburg, Arbeitsbereiche Schiffbau, Report Nr. 591.
13. Hwang, D. H., Rörup, J., Lee, J. W., 1998, On the Fatigue Strength Assessment of Double Hull Structure Member, 1998, 98' Annual Autumn Meeting of SNAK, Inchon, Korea